Observation of Mutiphoton Absorptions in Laser-Assisted Electron Scattering in a Femtosecond Intense Laser Field

Kakuta Ishida, Yuya Morimoto, Reika Kanya, and Kaoru Yamanouchi
Department of Chemistry, School of Science, The University of Tokyo, Japan
kakuta@chem.s.u-tokyo.ac.jp

Abstract: High-order multiphoton laser-assisted electron scattering processes induced by collision of electrons and Xe atoms in a femtosecond intense laser filed were observed for investigating high-order laser-atom interactions.

OCIS codes: (020.0020) Atomic and molecular physics; (020.2649) Strong filed laser physics

1. Introduction

When electrons are scattered by an atom in a laser field, the energy of the scattered electrons can be shifted by $n\hbar\omega$ (n: an integer, $\hbar\omega$: photon energy). This phenomenon is called laser-assisted electron scattering (LAES). Since 1970s, the LAES processes occurring in a relatively weak laser field ($I < 10^9$ W/cm^2) have been experimentally investigated using mid-infrared CO_2 lasers (λ = 10.6 μm) [1], and the energy and angular distributions of the scattered electrons in the LAES processes were explained well by the Kroll-Watson theory (KWT) [2] in which the interaction between the target atom and the laser field is neglected. Recently, the LAES processes induced by an intense near-infrared laser field ($I > 10^{12}$ W/cm^2, λ = 800 nm) were observed for $n = \pm1$ processes [3] and $n = \pm1, \pm2, +3$ processes. In such an intense laser field in the near-infrared region, the laser-atom interaction cannot be neglected, and significant discrepancies from the KWT are expected in the angular distributions of the LAES signals as predicted by several theoretical studies [4,5]. Because the discrepancies in the high-n LAES processes carry information on the temporal evolution of the electron cloud oscillating at nth-order harmonic of the laser carrier frequency, measurements of the high-n LAES processes in the near-infrared region will provide us with fundamental understanding of highly-nonlinear interactions between the laser field and the electron cloud within the target atom. In the present study, we report the first observation of the high-n LAES processes in the wide n range, n = +1 ~ +6, induced by a near-infrared intense laser field.

2. Experimental setup

The details of the experimental setup are described in Ref. [6]. An electron beam pulse (1 keV, Δt = 19 ps) collides with a Xe gas in a femtosecond intense laser field (λ = 800 nm, Δt = 100 fs, $I = 8.8\times10^{12}$ W/cm^2). The scattered electrons are introduced into a toroidal-type electron energy analyzer, and the energy and angular distributions of the scattered electrons are resolved and detected by a two dimensional imaging detector. The unscattered and scattered electrons in the range of $\theta < 2$ degrees are blocked by a Faraday cup placed in front of the energy analyzer. In this measurement, a typical count rate of the elastic scattering signals is around 300 cps, and the net accumulation time is around 156 hours. The energy resolution of the setup is around 0.6 eV, which is sufficiently high for resolving the energy shifts by the photon energy of the laser light (1.55 eV).

3. Results and Discussion

The obtained raw images of scattered electrons are shown in Fig. 1. Figure 1(a) shows the signals of scattered electrons obtained when the scattering occurred in the laser field, while Fig. 1(b) shows the background signals

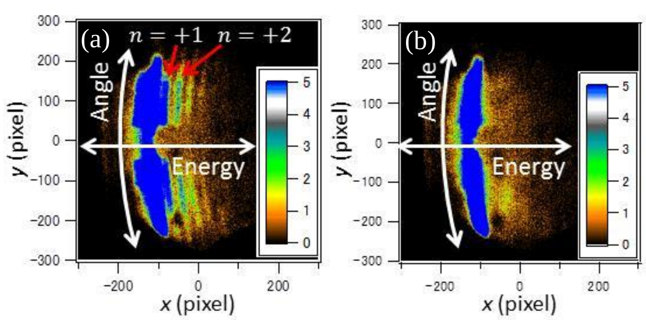

Fig. 1. Raw images of the electrons scattered by Xe atoms. (a) Signals with the laser field. (b) Background signals.

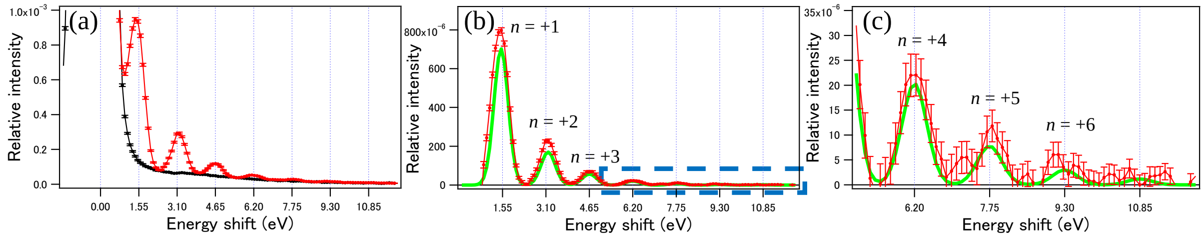

Fig. 2. (a) Energy spectra of the electrons scattered by Xe atoms. The signal intensities are normalized by the peak intensity of the elastic scattering signals with the laser field. Red dots: scattering signals with the laser field. Black dots: background signals. (b) Subtraction of the background signals from the signals with the laser field. Red dots: experimental results. Green solid line: simulated relative intensities of the LAES signals. (c) Expanded view of the region indicated by the broken box in Fig. 2(b).

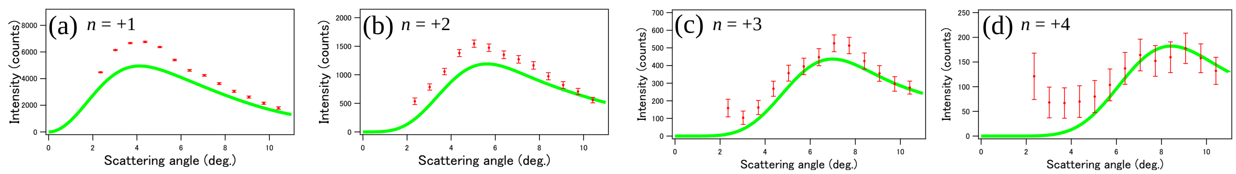

Fig. 3. Angular distributions of LAES signals for the (a) n = +1, (b) n = +2, (c) n = +3, and (d) n = +4 transitions. Red dots: observed LAES signals. Green solid line: numerical calculation by KWT.

obtained when the temporal delay of the electron beam pulse from the laser beam pulse was set to be 300 ps, so that the scattering occurs without the influence of the laser field. The net accumulation time was around 78 hours for both images. As shown by the white arrows, vertical and horizontal directions show the angular and energy distributions, respectively. Intense elastic scattering signals forming arcuate lines are seen in both Figs. 1(a) and (b), but additional weak arcuate lines on the right side of the intense arcuate line can only be seen in Fig. 1(a) as pointed by the red arrows. Figure 2(a) shows the energy spectra obtained from Figs. 1(a) and (b). Sideband structures with the spacing of 1.55 eV are clearly seen in the energy spectrum of electrons scattered in the laser field (red dots). The red dots in Fig. 2(b) show an energy spectrum of the background-subtracted LAES signals, and Fig. 2(c) shows the expanded view of the region indicated by the broken box in Fig. 2(b). By the subtraction of the background signals, the six distinct peaks assigned to the LAES processes with n = +1, +2, +3, +4, +5, and +6 appear as shown in Fig. 2(b) and (c), and the simulated relative intensities of the LAES signals (green solid lines) are in good agreement with the experimental results.

The angular distributions of electron signals for the multiphoton LAES processes (n = +1, +2, +3, and +4) are shown in Figs. 3(a), (b), (c), and (d), respectively. While general tendencies of the angular distributions are reproduced by those obtained by numerical calculations based on the KWT, significant discrepancies between the experimental results and the results of numerical calculations are identified in all the subfigures in Fig. 2.

As discussed above, deviations from the KWT can be ascribed to the laser-atom interaction. However, the discrepancies appearing in Figs. 3 are found to be even larger than the corrections made by the theory in which the laser-atom interaction is taken into account [4]. The largest deviation from the estimation by the KWT identified for n = +1 may indicate that the experimental laser field intensity is overestimated because the relative intensity of the LAES signals for n = +1 is expected to become larger than those for $n > 1$ when the laser filed intensity decreases. For more quantitative discussions of the discrepancies from the KWT in the angular distributions of LAES signals, more precise measurements of temporal profiles of the laser pulses as well as more careful electron signal accumulations under constant experimental conditions are required.

4. References

[1] N. J. Mason, "Laser-assisted electron-atom collisions," *Rep. Prog. Phys.* **56**, 1275-1346 (1993).

[2] N. M. Kroll and K. M. Watson, "Charged-Particle Scattering in the Presence of a Strong Electromagnetic Wave," *Phys. Rev. A* **8**, 804-809 (1973).

[3] R. Kanya, Y. Morimoto, and K. Yamanouchi, "Observation of Laser-Assisted Electron-Atom Scattering in Femtosecond Intense Laser Fields," *Phys. Rev. Lett.* **105**, 123202 (2010).

[4] B. A. Zon, "Bremsstrahlung in collisions between electrons and atoms," *Sov. Phys. JETP* **46**, 65-68 (1977).

[5] F. W. Byron Jr. and C. J. Joachain, "Electron-atom collisions in a strong laser field," *J. Phys. B* **17**, L295-L301 (1984).

[6] R. Kanya, Y. Morimoto, and K. Yamanouchi, "Apparatus for laser-assisted electron scattering in femtosecond intense laser fields," *Rev. Sci. Instrum.* **82**, 123105 (2011).